12-2015

Impact of changes in GRACE derived terrestrial water storage on vegetation growth in Eurasia

G. A.

I. Velicogna

John S. Kimball
University of Montana - Missoula

Y. Kim

Recommended Citation

Velicongna, I., Kimball J. S., and Kim Y. (2015). Impact of changes in GRACE derived terrestrial water storage on vegetation growth in Eurasia. Environmental Research Letters, 10(12): 10 pp., doi: 10.1088/1748-9326/10/12/124024

Impact of changes in GRACE derived terrestrial water storage on vegetation growth in Eurasia

Environmental Research Letters

LETTER

Impact of changes in GRACE derived terrestrial water storage on vegetation growth in Eurasia

G A[1], I Velicogna[1,2], J S Kimball[3] and Y Kim[3]

[1] Department of Earth System Science, University of California Irvine, CA, USA
[2] Jet Propulsion Laboratory, California Institute of Technology Pasadena, CA, USA
[3] Numerical Terradynamic Simulation Group, College of Forestry & Conservation, University of Montana, Missoula, MT, USA

E-mail: geruoa@uci.edu

Keywords: water cycle, terrestrial water storage, satellite remote sensing, GRACE, ecosystem

Supplementary material for this article is available online

OPEN ACCESS

RECEIVED
3 August 2015

REVISED
10 November 2015

ACCEPTED FOR PUBLICATION
11 November 2015

PUBLISHED
29 December 2015

Abstract

We use GRACE-derived terrestrial water storage (TWS) and ERA-interim air temperature, as proxy for available water and temperature constraints on vegetation productivity, inferred from MODIS satellite normalized difference vegetation index (NDVI), in Northern Eurasia during 2002–2011. We investigate how changes in TWS affect the correlation between NDVI and temperature during the non-frozen season. We find that vegetation growth exhibits significant spatial and temporal variability associated with varying trend in TWS and temperature. The largest NDVI gains occur over boreal forests associated with warming and wetting. The largest NDVI losses occur over grasslands in the Southwestern Ob associated with regional drying and cooling, with dominant constraint from TWS. Over grasslands and temperate forests in the Southeast Ob and South Yenisei, wetting and cooling lead to a dominant temperature constraint due to the relaxation of TWS constraints. Overall, we find significant monthly correlation of NDVI with TWS and temperature over 35% and 50% of the domain, respectively. These results indicate that water availability (TWS) plays a major role in modulating Eurasia vegetation response to temperature changes.

1. Introduction

High latitude boreal and Arctic biomes are changing in response to recent climatic warming (Overland *et al* 2008). Recent atmospheric CO_2 anomalies, satellite normalized difference vegetation index (NDVI) records, satellite data driven vegetation productivity estimates, and ground-based observations indicate regional declines in Northern ecosystem productivity since the mid-1990s that may be a biophysical response to temperature induced drought stress (Zhang *et al* 2007, Piao *et al* 2008, Ma *et al* 2012, Yi *et al* 2013). A diverse response of Northern ecosystems to regional warming and drought has been reported from limited field experiments (Lloyd and Bunn 2007, Schwalm *et al* 2010, Yi *et al* 2010, Peng *et al* 2011, Tei *et al* 2015), while extension of these findings to the pan-boreal/Arctic region is constrained by the limited extent of these studies and a sparse regional measurement network. During the past 30 years, published studies have shown positive correlation between vegetation productivity and temperature changes during the growing season in the Arctic (e.g. Zhou *et al* 2001, Lucht *et al* 2002), however, more recent studies suggest a weakening of this relationship (e.g. Buermann *et al* 2014, Piao *et al* 2014), indicating complex patterns of change in vegetation growth in relation to regional temperature trends, including predominant greening in tundra areas, and widespread productivity declines in boreal forests attributed to water stress (Zhang *et al* 2008, Bhatt *et al* 2010, 2013, Beck and Goetz 2011, Ma *et al* 2012, Berner *et al* 2013, Buermann *et al* 2014, Guay *et al* 2014, Walker and Johnstone 2014). It is difficult to evaluate trends in vegetation response to water constraints at Northern high latitudes, because of uncertainty in regional precipitation and other water budget indicators due to intrinsic bias in available satellite and reanalysis data, and sparse ground measurements (Serreze *et al* 2006, Zhang *et al* 2009, Rawlins *et al* 2010). Satellite-derived soil moisture estimates have large uncertainties in the

Northern regions (Mladenova *et al* 2014). In fact satellite soil moisture retrieval errors are large due to the presence of snow, ice, surface water and dense canopies (Naeimi *et al* 2012, Högström *et al* 2014). In previous studies, local and regional responses of vegetation to moisture variability have typically been inferred indirectly from correlations with model based temperature and precipitation, or atmosphere vapor pressure deficit (e.g. Nemani *et al* 2003, Zhang *et al* 2008), or from reanalysis based moisture indices (e.g. Berner *et al* 2013).

Since 2002 GRACE satellite measurements have provided regional estimates of monthly changes in terrestrial water storage (TWS) (Swenson *et al* 2006, Reager and Famiglietti 2009, Famiglietti *et al* 2011), i.e. of water content both on and below the land surface. GRACE data provide a unique tool for observing trends in water availability (Rodell *et al* 2009, Velicogna *et al* 2012). These data have been used to investigate regional climate variability, including drought related impacts (Chen *et al* 2013, Thomas *et al* 2014), and to study water constraints on vegetation growth in Australia (Yang *et al* 2014). In Eurasia, previous studies have shown that GRACE TWS changes are consistent with observed changes in net precipitation (Landerer *et al* 2010, Velicogna *et al* 2012).

Here we investigate the vegetation response to temperature changes and water storage availability from 2002 to 2011 in the Ob, Yenisei and Lena basins, which constitute 70% of all riverine freshwater inputs to the Arctic Ocean (Gordeev *et al* 1996). To study the relationship between vegetation growth and water storage and temperature changes, we use MODIS NDVI, GRACE TWS estimates, and ECMWF (European Centre for Medium-Range Weather Forecasts) ERA-Interim 2 m air temperature (Dee *et al* 2011). We discuss the rationale of using GRACE TWS as a proxy for plant available water supply. We study the spatial pattern of trends in NDVI, TWS, and temperature (T) and evaluate the trend and inter-annual relation of NDVI changes with temperature and water availability during 2002–2011. We conclude on discussing the role of water storage, as a proxy for plant-available water supply, in modulating the impact of temperature changes on regional vegetation productivity in Northern ecosystems.

2. Data and methodology

We use 113 monthly GRACE solutions from the Center for Space Research at the University of Texas (Tapley *et al* 2004), between August 2002 and December 2011. Each gravity solution consists of spherical harmonic coefficients, C_{lm} and S_{lm}, up to degree, l, and order, m, 60. We use monthly values of $\mathbf{C}_{20}$ coefficients from satellite laser ranging (Cheng *et al* 2013) and include degree-1 coefficients calculated as described by Swenson *et al* (2008). The GRACE data directly measure monthly TWS changes, because this is the largest source of mass change within our area of interest; other mass changes such as glacial isostatic adjustment (GIA) are of much lower magnitude. TWS anomalies are calculated relative to the period August 2002–December 2011. To separate seasonal variability from inter-annual variability and trends we apply a 13 month smoothing to the GRACE monthly Stokes coefficients. To do this for each 13 month window, we simultaneously solve for annual, semiannual, 3 month period signals, a constant and a linear trend. We assign the sum of the constant term and the linear trend to the center point (i.e., the 7th month) of each time window. This moving average scheme yields a smoothed time series where all seasonal variations are removed. This smoothing procedure is not applied to the first and last 6 months of record because a one-year cycle is required to extract the seasonal signal. The GRACE data are also corrected for the GIA signal following Paulson *et al* (2007). To reduce the random error components, we apply a Gaussian smoothing with a 400 km radius (Wahr *et al* 1998) and then we generate monthly evenly spaced latitude–longitude grid. Linear trends are calculated using these monthly maps.

Water in seasonal snow cover is not directly available for vegetation growth. We therefore remove estimates of snow storage from the GRACE monthly TWS time series. We estimate the snow cover contribution using 25 km EASE-Grid monthly satellite derived snow water equivalent (SWE) data from the Advanced Microwave Scanning Radiometer on EOS Aqua, AMSR-E, (http://nsidc.org/data/amsre/) (Derksen *et al* 2003). The SWE retrieval accuracy is generally higher over flatter land areas with less vegetation cover. This is the case of the analyzed region that has relatively flat topography and is mainly covered by grassland, boreal taiga and tundra vegetation cover. Velicogna *et al* (2012) found good agreement between changes in snow mass from the AMSR-E SWE record and station-based cold season precipitation trends for the region. We use these data to remove the SWE signal from the GRACE TWS estimates. We only remove the SWE of the non-melted snow; hence the residual TWS includes the water storage from melted snow. In the remainder of the paper, TWS refers to the signal corrected for SWE.

In principle, the SWE-corrected GRACE TWS includes components such as groundwater that is not directly within the vegetation root zone. These other components vary on longer time scales, whereas short time scale (e.g. monthly) variations in water storage are related to soil water changes linked to vegetation growth (Vicente-Serrano *et al* 2010, 2013). In addition, previous studies have shown that in Eurasia, variations in SWE-corrected GRACE TWS are strongly correlated with net precipitation at the monthly and inter-annual time scale (Landerer *et al* 2010, Velicogna *et al* 2012), which has also been used as a proxy for

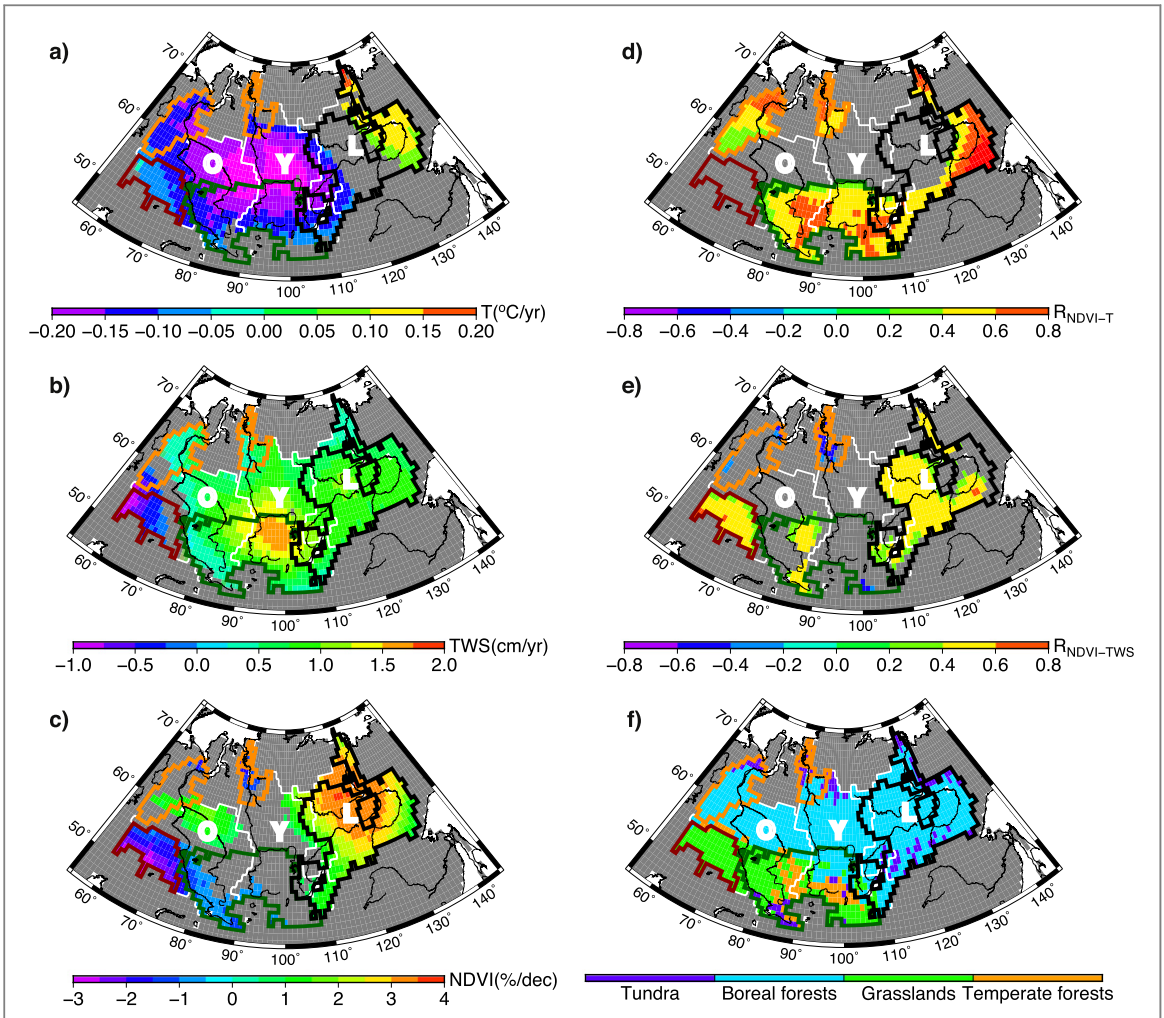

Figure 1. Linear trends for (a) temperature (T) in degree C yr^{-1}, (b) terrestrial water storage (TWS) in cm yr^{-1}, (c) normalized difference vegetation index (NDVI) in %/decade and correlation coefficients for (d) T and NDVI (R_{NDVI-T}); and (e) TWS and NDVI ($R_{NDVI-TWS}$) for the non-frozen season during the analyzed period. Only regions with a statistically significant correlation ($p < 0.02$) are shown. (f) Land cover types in the three river basins. White lines are the boundaries of the Lena (L), Yenisei (Y) and Ob (O) river basins. Also shown are contour lines for region 1 (dark red), region 2 (dark green), region 3 (black) and region 4 (dark orange).

water available for plant growth. Therefore we use the monthly SWE-corrected GRACE TWS estimates as a surrogate for plant-available water supply.

We use ERA-Interim monthly 2 m height temperature (T) (Dee *et al* 2011) and MODIS derived NDVI records. The NDVI from satellite optical-IR remote sensing is sensitive to vegetation canopy greenness and has been used as a surrogate indicator of photosynthetic canopy growth changes over Northern land areas (Bogaert *et al* 2002, Goetz *et al* 2005). We use a monthly composited MODIS-MOD13Q1 NDVI dataset with $1^{\circ} \times 1^{\circ}$ spatial resolution (Huete *et al* 2011) to define vegetation canopy changes over the study domain. All datasets are processed as the GRACE data, i.e. anomalies are calculated relative to the common period (August 2002–December 2011), converted to spherical harmonics, truncated to degree 60, spatially averaged using a 400 km smoothing and converted back to the spatial domain on a regular 1° longitude–latitude grid. We calculate TWS, T, and NDVI trends. Trends are considered statistically significant when they exceed the respective $1-\sigma$ error (figure 1). We use the global Earth System Data Record of daily landscape freeze-thaw status derived from satellite microwave remote sensing to define daily landscape freeze-thaw status over all Northern vegetated land areas (Kim *et al* 2011). For each year, we define the non-frozen (NF) season at each grid cell as described in Kim *et al* (2014).

To investigate the impact of temperature and water storage changes on vegetation growth, we examine the partial correlation between NDVI and T (NDVI–T correlation) and NDVI and TWS (NDVI–TWS correlation) for the NF season. The partial correlation removes the inter-dependency between T and TWS. This study focuses on the relationship between trends and inter-annual NDVI variations with T and TWS. The trends and inter-annual changes are small compared to the seasonal variability, hence before calculating the partial correlations, we remove the seasonal signal from each time series as described earlier; otherwise it would dominate the correlation analysis.

In the remainder of the paper, we use R_{NDVI-T} and $R_{NDVI-TWS}$ to indicate the NF season partial correlation between NDVI and T and between NDVI and TWS, respectively. To identify whether trend or inter-annual variability is driving the correlations we calculated the correlations for de-trended time series and compare them with the one for the original time series.

Due to the spatial resolution of the GRACE data, TWS estimates can only be used to study vegetation growth changes at the regional scale, i.e. $\geqslant$400 km. To facilitate the interpretation of the results, we divide the study domain into a set of four regions. Each region corresponds to an area with significant NDVI–T or NDVI–TWS correlation and with a consistent trend in NDVI (figures 1(c)–(e)). Within each region, we analyze the spatially averaged correlation coefficients R_{NDVI-T} and $R_{NDVI-TWS}$ to determine the primary moisture or temperature constraints and we discuss the results as a function of vegetation type within the region.

Change in fire disturbance regime also influence vegetation growth patterns and may affect our results based on correspondence between TWS, T and NDVI. To evaluate the impact of fire on vegetation growth, we use area burned data from the fourth-generation global fire emissions database (Giglio *et al* 2013) and for each vegetation type we compare NDVI trends on burned and unburned areas.

3. Results

Figures 1(a)–(c) shows the T, TWS and NDVI trend for the NF season during 2002–2011. We find overall cooling in the Ob and Yenisei basins (figure 1(a)), and warming in most of the Lena basin, with the largest warming in the East. TWS increases in the Lena and Yenisei basins, with larger rates near the center of each basin (figure 1(b)). TWS increases in the North (N) and East (E) Ob basin, and decreases in the Southwest (SW). NDVI increases in the Lena, E Yenisei and N Ob basins, and declines in the South (S) Ob basin, and SW Yenisei. The NDVI changes in the Yenisei are generally small or not significant (figure 1(c)). Figures 1(d)–(e) show R_{NDVI-T} and $R_{NDVI-TWS}$ calculated for the entire analyzed region; however, in our analysis we consider only areas where the partial correlation coefficient is statistically significant at more than 98% confidence level ($p < 0.02$). We identify climatic constraints on vegetation activity for 68% of the analyzed region. In the remaining 32% of the region, we do not find significant correlation between NDVI and T or NDVI and TWS.

Within the analyzed domain, NDVI correlates well ($p < 0.02$) with TWS and T over 35% and 50% of the area, respectively. $R_{NDVI-TWS}$ is positive ($p < 0.02$) in W and N Lena, SE Yenisei and SW and SE Ob basins (figure 1(e)) and is not significant elsewhere. We find a positive R_{NDVI-T} in the E Lena (with R_{NDVI-T} 35% larger than $R_{NDVI-TWS}$), N and SE Ob (with R_{NDVI-T} 29% larger than $R_{NDVI-TWS}$ in SE Ob), and S Yenisei basins (figure 1(d)). By comparing partial correlation results for the de-trended and original time series, we find that over the entire domain, the NDVI–T correlation is mostly driven by the inter-annual variability. In contrast, for the NDVI–TWS correlation, we find that in the Lena basin, the correlation is driven by the trend, whereas in the SW Ob basin, is driven by both the trend and the inter-annual variability, and in the SE Ob by the inter-annual variability.

Table 1. Summary of results obtained comparing NDVI, total water storage (TWS) and temperature in the four identified regions[a].

	Region 1	Region 2	Region 3	Region 4
Tundra	0%	8.3%	13%	24%
Boreal forest	1.4%	23%	83%	76%
Grasslands	97%	44%	3.4%	0%
Temperate forest	1.3%	24%	0.7%	0%
$R_{NDVI-TWS}$ ($p < 0.02$)	100%	21%	73%	0%
R_{NDVI-T} ($p < 0.02$)	0%	100%	60%	100%
T (°C)	10.9	10.4	7.5	5.3
P (mm)	412	494	468	574

[a] Areal proportion (%) of different land cover types and of significant ($p < 0.02$) NDVI–TWS correlation ($R_{NDVI-TWS}$) and NDVI–T correlation (R_{NDVI-T}) for regions 1–4. Also included are mean temperature (T) and mean annual precipitation (P) for the non-frozen seasons during the analyzed period from ERA-Interim reanalysis (Dee *et al* 2011).

Spatially averaged NDVI–T and NDVI–TWS correlations ($p < 0.02$) and the land cover partitioning for the four identified regions are summarized in table 1. The identified dominant water and temperature constraints are summarized in figure 2. The time series of NDVI, T and TWS are shown in figure S2. We then use these results to calculate the areal proportion of relative water and temperature constraints for each vegetation type in the entire analyzed domain (table 2).

Region 1, the SW Ob basin, is cooling and drying, with a significant decrease in NDVI (figures 1(a)–(c). The land cover in this region predominantly consists of relatively arid grassland (97%) (table 1). $R_{NDVI-TWS}$ is positive over the entire region (average $R_{NDVI-TWS} = 0.48$, $p < 0.02$), while R_{NDVI-T} is not significant. These results are consistent with a regional dominance of TWS constraints on vegetation productivity.

Region 2 covers the SE Ob and S Yenisei basins, and has a mixed land cover of 44% grassland, 24% temperate forest, 23% boreal forest and 8% tundra. The region accounts for 83% of the temperate forest and 53% of the grassland biomes of the entire study domain. This area is cooling and wetting, with a small negative NDVI trend significant only in the South (figures 1(a)–(c). R_{NDVI-T} is positive (average $R_{NDVI-T} = 0.53$, $p < 0.02$) over the entire region,

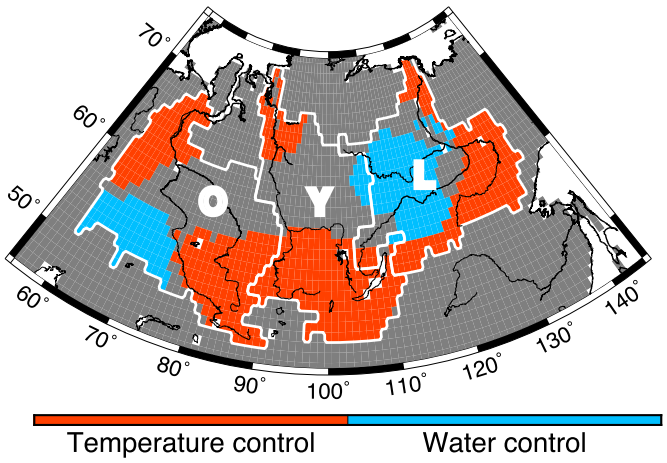

Figure 2. Identified water (blue) and temperature (red) control on vegetation growth.

Table 2. Results showing the percentage of areas where we find dominant temperature or water controls on vegetation growth. Unidentified regions are where neither temperature nor water supply is the dominant control. Column 2 shows the areal proportions relative to the entire analyzed area. Columns 3–6 show the areal proportions relative to each land cover type.

	Areal proportions	Tundra	Boreal forests	Grasslands	Temperate forests
Temperature control	50%	74%	40%	58%	83%
Water control	18%	8%	17%	32%	1%[a]
Unidentified	32%	18%	43%	10%	16%

[a] There are 26% of temperate forest showing significant NDVI–TWS correlation. But most of those located in SE Ob are counted as temperature control as R_{NDVI-T} there is 33% larger than $R_{NDVI-TWS}$. Therefore only 1% of the total temperate forest shows dominating water control.

$R_{NDVI-TWS}$ is significant in the temperate forest area in SE Ob ($R_{NDVI-TWS} = 0.35$, $p < 0.02$). Here, T is the primary constraint on vegetation productivity.

Region 3 (figure 1) includes almost the entire Lena basin and small portions of the NE and SE Yenisei. These two small areas are included here rather than in region 2 as they show an increase in NDVI consistent with the trend in region 3. Here the land cover is composed of boreal forest (83%), tundra (13%) and grassland (3%). The entire region shows TWS wetting, but with a spatially variable temperature trend: the E Lena basin is warming, the NE and SE Yenisei are cooling, and there is no significant T trend in the rest of the region (figures 1(a)–(b). In the E Lena basin, the average $R_{NDVI-TWS}$ and R_{NDVI-T} are 0.46 and 0.61, respectively. R_{NDVI-T} is 33% larger than $R_{NDVI-TWS}$, indicating, in agreement with Piao *et al* (2011), that T has a generally stronger impact on vegetation in this region. In the remaining portion of the basin and in the NE Yenisei, however, $R_{NDVI-TWS}$ is positive (average $R_{NDVI-TWS}$ in these areas is 0.46, $p < 0.02$), and the NDVI–T correlation is not significant. Here we observe an NDVI greening response to TWS wetting, indicating a dominant TWS constraint to vegetation activity.

The SE-Yenisei consists mostly of boreal forest (69%) and grassland (17%). This area is cooling and wetting, and features a small NDVI increase (1.2%/decade on average, $p < 0.32$). R_{NDVI-T} is positive (average $R_{NDVI-T} = 0.53$, $p < 0.02$) and 29% larger than the $R_{NDVI-TWS}$ (average $R_{NDVI-TWS} = 0.41$, $p < 0.02$). Here temperature is the main constraint on vegetation growth.

Region 4 includes a portion of the NW Ob basin and a small area in the N Yenisei. Boreal forest and tundra cover 76% and 24% of the area, respectively (table 1). This region features a decreasing T trend, a small increase in TWS and no significant NDVI trend (figures 1(a)–(c)). R_{NDVI-T} is positive (average $R_{NDVI-T} = 0.51$, $p < 0.02$) over the entire region, while the TWS–NDVI correlation is not significant (table 1), indicating an overall T constraint.

Overall the analyzed domain includes 63% boreal forests, 20% grasslands, 10% tundra and 7% temperate forests. Within the tundra (figure 1(f)), NDVI is significantly ($p < 0.02$) correlated with T in 74% of the region and with TWS in only 8% ($p < 0.02$) (table 2), suggesting cold temperature as the main constraint on vegetation growth. We find no significant correlation in 18% of tundra. Boreal forests show a diverse response to climatic variations; significant correlation of NDVI with T and TWS occur over 40% and 17% of boreal areas, respectively, and no correlation elsewhere (table 2). Overall temperature-constrained boreal forests are distributed over the NW Ob, SE Yenisei and E Lena, while TWS-constrained biomes

are found in the central and W Lena. Grasslands also show mixed climatic controls. TWS is the dominant constraint on NDVI growth in the SW Ob basin where we observe cooling and drying; this area accounts for 32% of the grasslands. While in the SE Ob and S Yenisei, where we observe cooling and wetting, we find significant correlation with T; these regions account for 58% of the grasslands. The analyzed domain also includes a relatively small area of temperate forests (S Ob and S Yenisei); 83% of this area shows significant NDVI–T correspondence, indicating a primary cold temperature constraint in temperate forests.

When we evaluate the impact of fire disturbance on vegetation growth, we find mean annual burned area of 1.9% in grassland, and less than 0.5% for the other land covers in the analyzed domain. Over the grassland, we find similar NDVI trends ($\sim -2\%$/decade) in both burned and unburned areas, indicating that fire at the regional scale is not a dominant factor controlling vegetation growth, consistent with previous studies in Eurasia (Buermann *et al* 2014).

4. Discussion

During the analyzed period, the greatest NDVI gains occur where we observe warming and wetting trends, and boreal forest is the locally dominant biome (Lena basin, region 3, average NDVI trend = 2.4%/decade). The greatest NDVI losses are associated with cooling and drying trends, and occur in regions dominated by grassland (74%) (SW Ob basin, region 1, average NDVI trend = −1.9%/decade). NDVI changes are small or not significant in regions that are cooling and wetting. Our study domain does not sample warming and drying condition, but it is likely that warming would exacerbate drying-induced TWS constraints and reduce NDVI. The spatial pattern of these changes provides an indication of how regional vegetation growth may respond to future climate conditions.

Regional climate model (IPCC AR5) projections indicate warmer climate conditions over Eurasia (e.g. Miao *et al* 2014), and an overall increase in precipitation with possible drying trends in the Southern regions (Monier *et al* 2013, Sillmann *et al* 2013). Our results imply that projected warmer, wetter trends could promote widespread productivity increases and conditions more suited to temperate forest than colder boreal and tundra areas; however, where warmer, drier conditions occur we may expect to see productivity declines and conditions better suited to drought tolerant grassland over tundra and forested areas (Wang and Overland 2004, Lenton *et al* 2008).

Our results indicate that fire, at the regional scale, is not a dominant factor controlling vegetation growth, consistent with previous studies in Eurasia (Buermann *et al* 2014). However, area burned and fire severity have been increasing in Eurasia for the last decade (Soja *et al* 2007, Hayes *et al* 2011) and with projected warmer and possible drier conditions in Southern Eurasia, fire disturbance is likely to have an increasing impact on the regional ecosystem (Tchebakova *et al* 2009).

Most of the Lena and a large portion of the Yenisei basins are underlain by permafrost (Brown *et al* 1997, Zhang *et al* 2005). Permafrost degradation may play a significant role in modulating the vegetation response to ongoing climate change in this region. Model projections predict shrinkage of the areal extent of permafrost and deepening of the active layer which has the potential to significantly impact plant-available soil moisture (Lawrence and Slater 2005, Anisimov 2007, Saito *et al* 2007, Lawrence *et al* 2008). The interaction between permafrost degradation, climate change and vegetation growth is a topic of ongoing research; the mechanism, timing and extent of this interaction is still uncertain (e.g. Tchebakova *et al* 2009, Walker *et al* 2009, Jorgenson *et al* 2010, 2013, Nauta *et al* 2014). Long-term monitoring is needed to determine if deepening of the active layer along with increasing drainage of root-zone soil water is leading to shifts in vegetation patterns and climatic control factors influencing productivity (e.g. Lawrence and Slater 2005, Jorgenson *et al* 2013).

During 2002–2011, T exerted a major constraint on NDVI over a large portion of Eurasian grassland and temperate forest areas, mostly in the SE Ob and S Yenisei basins, while previous studies, based on longer, multi-decadal observations, indicate that these biomes are mainly water limited (e.g. Piao *et al* 2011, Kim *et al* 2014). We attribute this difference to regional wetting and cooling trends, observed during the study period, that have been associated to a decadal and quasi-decadal climatic variability (Zhang *et al* 2007, 2012, Bhatt *et al* 2013), rather than a longer term climate change response (Cohen *et al* 2009, Piao *et al* 2011, Kim *et al* 2014). Our results indicate that the regional response of NDVI to temperature is influenced by TWS changes and associated water supply controls to vegetation growth. An observed increasing TWS trend is consistent with an apparent reduction in water supply constraints, so that T cooling represents the dominant constraint driving vegetation growth reductions in the region. These results are consistent with recent findings that soil moisture, as another water supply proxy, modulates temperature–productivity correlations and ecosystem net carbon uptake in Northern high latitude regions (Piao *et al* 2014, Yi *et al* 2014), while drought-induced water stress has been the dominant cause of observed reduction in vegetation growth for Canadian boreal forests (e.g. Ma *et al* 2012) despite regional warming and associated reductions in cold temperature constraints to productivity.

Summer cloud cover can also impact vegetation growth by limiting incident solar radiation on vegetation (Nemani *et al* 2003). Recent studies have linked changes in summer cloud to regional variability in

temperature trends and vegetation growth (Tang and Leng 2012, Bhatt *et al* 2013). Piao *et al* (2014) have shown that, in the study domain, the NDVI correlations with shortwave radiation are weaker than those with temperature or precipitation. Still increase in cloud cover, observed during the analyzed period, may have contributed to the negative NDVI–TWS correlation observed in the Southern and Northern end of the study domain (figure 1(e)) (e.g. Tang and Leng 2012). Future studies will incorporate additional observations to further investigate the relation between changes in TWS and summer cloud cover, and the related impact on vegetation growth.

Seasonal snow cover may affect vegetation growth as winter snow accumulation provides thermal insulation of soil and melting snow water provides water supply to vegetation growth in the NF seasons (Grippa *et al* 2005, Iijima *et al* 2010, Buermann *et al* 2013, Barichivich *et al* 2014, Yi *et al* 2014). In the central Lena the observed TWS increase is largely due to a multi-year increase in winter snowfall since 2004 (Iijima *et al* 2010). The annual maximum TWS occurs typically in May–June and it is related to the amount of snowmelt (Zhang *et al* 2012). In this region the NDVI–TWS correlation is driven by the trends, and we find a positive correlation ($R = 0.81$, $p < 0.01$) between annual maximum TWS and early NF season NDVI. This suggests that seasonal snow pack and water supply from snowmelt have an important influence on vegetation activity. Further study is needed to investigate this correlation.

Overall, we find that cold temperature constraints are the main influence on vegetation activity in 50% of the study domain, while water supply constraints are the dominant control on vegetation activity in 18% of the domain (table 2). GRACE data provide a regional unbiased estimate of TWS (e.g. Velicogna *et al* 2012) and an observation-based proxy for analyzing changing water supply controls to vegetation productivity. Longer TWS time series will be obtained from continuing GRACE and GRACE follow-on mission (scheduled launch August 2017) observations, enabling improved diagnosis of regional climate trends from large characteristic climate variability. New soil moisture observations from the NASA Soil Moisture Active Passive (SMAP) mission and continuing improvements to regional snow cover (SWE) datasets may enable further partitioning of GRACE based TWS into surface moisture changes directly affecting vegetation growth versus deeper groundwater that is less accessible to plants.

5. Conclusions

In this study we analyze satellite observations of monthly TWS changes from GRACE, and compare the results with MODIS NDVI and ERA-Interim T to clarify regional changes in vegetation productivity patterns and underlying water supply and temperature constraints over the three largest basins in Eurasia during 2002–2011. In agreement with previous studies, we observe large spatial and temporal heterogeneity in patterns of vegetation growth and underlying environmental controls (e.g. Zhang *et al* 2008, Beck and Goetz 2011, Buermann *et al* 2014). We find both greening and browning trends for tundra in Northern Eurasia, driven by temperature warming and cooling, respectively. In boreal forests, we identify an overall greening trend, caused by relaxation of cold temperature and water supply constraints. In temperate forest and grassland regions, cold temperature is the dominant climatic control due to the relaxation of water constraints. Overall, we find that recent changes in plant-available water (either decrease or increase in available water supply) are a critical factor modulating the sign and magnitude of the regional vegetation growth response to temperature changes. Despite the short length of the satellite record, we find complex patterns of NDVI growth response to T and TWS changes that follow large regional climate and land cover gradients and provide for a space-for-time based assessment of potential vegetation responses to future climatic conditions. Our results indicate that future vegetation changes in the region will increasingly depend on having an adequate moisture supply to support potential vegetation growth enabled by regional warming and associated relaxation of cold temperature constraints. Warmer and wetter conditions will likely promote an expansion of temperate forest areas and loss of tundra, while warmer and drier conditions may promote grassland expansion and loss of forests. However ongoing increase in atmospheric CO_2 will likely modify the radiation budget and alter present-day plant physiology, and future studies are needed to understand its impact on vegetation growth and the associated climatic constraints. Longer satellite observation records from GRACE and follow-on missions in combination with planned soil moisture observations from SMAP and satellite SWE will expand and improve our assessment of plant-available moisture changes and environmental trends.

Acknowledgments

This work was performed at UCI and JPL-Caltech. It was partially supported by the NASA's Cryosphere, Terrestrial Hydrology, IDS, MEASURES Programs, Gordon and Betty Moore Foundation (GBMF3269). Data used in this manuscript are available upon request to the authors. We thank two anonymous reviewers for their careful reviews.

References

Anisimov O A 2007 Potential feedback of thawing permafrost to the global climate system through methane emission *Environ. Res. Lett.* **2** 045016

Barichivich J, Briffa K, Myneni R, Schrier G, Dorigo W, Tucker C, Osborn T and Melvin T 2014 Temperature and snow-mediated moisture controls of summer photosynthetic activity in Northern terrestrial ecosystems between 1982 and 2011 *Remote Sens.* **6** 1390–431

Beck P S A and Goetz S J 2011 Satellite observations of high Northern latitude vegetation productivity changes between 1982 and 2008: ecological variability and regional differences *Environ. Res. Lett.* **6** 045501

Berner L T, Beck P S A, Bunn A G and Goetz S J 2013 Plant response to climate change along the forest-tundra ecotone in Northeastern siberia *Glob. Change Biol.* **19** 3449–62

Bhatt U, Walker D, Raynolds M, Bieniek P, Epstein H, Comiso J, Pinzon J, Tucker C and Polyakov I 2013 Recent declines in warming and vegetation greening trends over pan-arctic tundra *Remote Sens.* **5** 4229–54

Bhatt U S *et al* 2010 Circumpolar Arctic tundra vegetation change is linked to sea ice decline *Earth Interact.* **14** 1–20

Bogaert J, Zhou L, Tucker C J, Myneni R B and Ceulemans R 2002 Evidence for a persistent and extensive greening trend in Eurasia inferred from satellite vegetation index data *J. Geophys. Res.* **107** 4119

Brown J, Ferrians O J J, Heginbottom J A and Melnikov E S 1997 *Circum-Arctic Map of Permafrost and Ground-Ice Conditions, Scale 1:10 000 000* US Geological Survey, Washington, DC

Buermann W, Parida B, Jung M, MacDonald G M, Tucker C J and Reichstein M 2014 Recent shift in Eurasian boreal forest greening response may be associated with warmer and drier summers *Geophys. Res. Lett.* **41** 1995–2002

Buermann W, Bikash P R, Jung M, Burn D H and Reichstein M 2013 Earlier springs decrease peak summer productivity in North American boreal forests *Environ. Res. Lett.* **8** 024027

Chen Y, Velicogna I, Famiglietti J S and Randerson J T 2013 Satellite observations of terrestrial water storage provide early warning information about drought and fire season severity in the Amazon *J. Geophys. Res. Biogeosciences* **118** 495–504

Cheng M, Tapley B D and Ries J C 2013 Deceleration in the Earth's oblateness *J. Geophys. Res. Solid Earth* **118** 740–7

Cohen J, Barlow M and Saito K 2009 Decadal fluctuations in planetary wave forcing modulate global warming in late boreal winter *J. Clim.* **22** 4418–26

Dee D P *et al* 2011 The ERA-Interim reanalysis: configuration and performance of the data assimilation system *Q. J. R. Meteorol. Soc.* **137** 553–97

Derksen C, Walker A and Goodison B 2003 A comparison of 18 winter seasons of *in situ* and passive microwave-derived snow water equivalent estimates in Western Canada *Remote Sens. Environ.* **88** 271–82

Famiglietti J S, Lo M, Ho S L, Bethune J, Anderson K J, Syed T H, Swenson S C, de Linage C R and Rodell M 2011 Satellites measure recent rates of groundwater depletion in California's central valley *Geophys. Res. Lett.* **38** L03403

Giglio L, Randerson J T and van der Werf G R 2013 Analysis of daily, monthly, and annual burned area using the fourth-generation global fire emissions database (GFED4) *J. Geophys. Res. Biogeosciences* **118** 317–28

Goetz S J, Bunn A G, Fiske G J and Houghton R A 2005 Satellite-observed photosynthetic trends across boreal North America associated with climate and fire disturbance *Proc. Natl Acad. Sci. USA* **102** 13521–5

Gordeev V V, Martin J M, Sidorov I S and Sidorova M V 1996 A reassessment of the Eurasian river input of water, sediment, major elements, and nutrients to the Arctic Ocean *Am. J. Sci.* **296** 664–91

Grippa M, Kergoat L, Le Toan T, Mognard N M, Delbart N, Hermitte J L and Vicente-Serrano S M 2005 The impact of snow depth and snowmelt on the vegetation variability over central Siberia *Geophys. Res. Lett.* **32** 21412

Guay K C, Beck P S A, Berner L T, Goetz S J, Baccini A and Buermann W 2014 Vegetation productivity patterns at high Northern latitudes: a multi-sensor satellite data assessment *Glob. Change Biol.* **20** 3147–58

Hayes D J, Mcguire A D, Kicklighter D W, Burnside T J and Melillo J M 2011 The effects of land cover and land use change on the contemporary carbon balance of the Arctic and boreal terrestrial ecosystems of Northern Eurasia *Eurasian Arctic Land Cover and Land Use in a Changing Climate* ed G Gutman and A Reissell (Amsterdam, Netherlands: Springer) pp 109–36

Huete A, Didan K, van Leeuwen W, Miura T and Glenn E 2011 MODIS vegetation indices *Land Remote Sensing and Global Environmental Change* ed B Ramachandran *et al* (New York: Springer) vol 11, pp 579–602

Högström E, Trofaier A, Gouttevin I and Bartsch A 2014 Assessing seasonal backscatter variations with respect to uncertainties in soil moisture retrieval in siberian tundra regions *Remote Sens.* **6** 8718–38

Iijima Y, Fedorov A N, Park H, Suzuki K, Yabuki H, Maximov T C and Ohata T 2010 Abrupt increases in soil temperatures following increased precipitation in a permafrost region, central Lena River basin, Russia *Permafr. Periglac. Process.* **21** 30–41

Jorgenson M T, Romanovsky V, Harden J, Shur Y, O'Donnell J, Schuur E A G, Kanevskiy M and Marchenko S 2010 Resilience and vulnerability of permafrost to climate change *Can. J. For. Res.* **40** 1219–36

Jorgenson T M *et al* 2013 Reorganization of vegetation, hydrology and soil carbon after permafrost degradation across heterogeneous boreal landscapes *Environ. Res. Lett.* **8** 035017

Kim Y, Kimball J S, Zhang K, Didan K, Velicogna I and McDonald K C 2014 Attribution of divergent Northern vegetation growth responses to lengthening non-frozen seasons using satellite optical-NIR and microwave remote sensing *Int. J. Remote Sens.* **35** 3700–21

Kim Y, Kimball J S, Mcdonald K C and Glassy J 2011 Developing a global data record of daily landscape freeze/thaw status using satellite passive microwave remote sensing *IEEE Trans. Geosci. Remote Sens.* **49** 949–60

Landerer F W, Dickey J O and Güntner A 2010 Terrestrial water budget of the Eurasian pan-Arctic from GRACE satellite measurements during 2003–2009 *J. Geophys. Res.* **115** D23115

Lawrence D M and Slater A G 2005 A projection of severe near-surface permafrost degradation during the 21st century *Geophys. Res. Lett.* **32** L24401

Lawrence D M, Slater A G, Romanovsky V E and Nicolsky D J 2008 Sensitivity of a model projection of near-surface permafrost degradation to soil column depth and representation of soil organic matter *J. Geophys. Res.* **113** F02011

Lenton T M, Held H, Kriegler E, Hall J W, Lucht W, Rahmstorf S and Schellnhuber H J 2008 Tipping elements in the Earth's climate system *Proc. Natl Acad. Sci. USA* **105** 1786–93

Lloyd A H and Bunn A G 2007 Responses of the circumpolar boreal forest to 20th century climate variability *Environ. Res. Lett.* **2** 045013

Lucht W, Prentice I C, Myneni R B, Sitch S, Friedlingstein P, Cramer W, Bousquet P, Buermann W and Smith B 2002 Climatic control of the high-latitude vegetation greening trend and Pinatubo effect *Science* **296** 1687–9

Ma Z, Peng C, Zhu Q, Chen H, Yu G, Li W, Zhou X, Wang W and Zhang W 2012 Regional drought-induced reduction in the biomass carbon sink of Canada's boreal forests *Proc. Natl Acad. Sci. USA* **109** 2423–7

Miao C, Duan Q, Sun Q, Huang Y, Kong D, Yang T, Ye A, Di Z and Gong W 2014 Assessment of CMIP5 climate models and projected temperature changes over Northern Eurasia *Environ. Res. Lett.* **9** 055007

Mladenova I E *et al* 2014 Remote monitoring of soil moisture using passive microwave-based techniques—theoretical basis and overview of selected algorithms for AMSR-E *Remote Sens. Environ.* **144** 197–213

Monier E, Sokolov A, Schlosser A, Scott J and Gao X 2013 Probabilistic projections of 21st century climate change over Northern Eurasia *Environ. Res. Lett.* **8** 045008

Naeimi V, Paulik C, Bartsch A, Wagner W, Kidd R, Park S E, Elger K and Boike J 2012 ASCAT surface state flag (SSF): extracting information on surface freeze/thaw conditions from backscatter data using an empirical threshold-analysis algorithm *IEEE Trans. Geosci. Remote Sens.* **50** 2566–82

Nauta A L *et al* 2014 Permafrost collapse after shrub removal shifts tundra ecosystem to a methane source *Nat. Clim. Change* **5** 24–7

Nemani R R, Keeling C D, Hashimoto H, Jolly W M, Piper S C, Tucker C J, Myneni R B and Running S W 2003 Climate-driven increases in global terrestrial net primary production from 1982 to 1999 *Science* **300** 1560–3

Overland J E, Wang M and Salo S 2008 The recent Arctic warm period *Tellus* A **60** 589–97

Paulson A, Zhong S and Wahr J 2007 Inference of mantle viscosity from GRACE and relative sea level data *Geophys. J. Int.* **171** 497–508

Peng C, Ma Z, Lei X, Zhu Q, Chen H, Wang W, Liu S, Li W, Fang X and Zhou X 2011 A drought-induced pervasive increase in tree mortality across Canada's boreal forests *Nat. Clim. Change* **1** 467–71

Piao S *et al* 2008 Net carbon dioxide losses of Northern ecosystems in response to autumn warming *Nature* **451** 49–52

Piao S *et al* 2014 Evidence for a weakening relationship between interannual temperature variability and Northern vegetation activity *Nat. Commun.* **5** 5018

Piao S, Wang X, Ciais P, Zhu B, Wang T and Liu J 2011 Changes in satellite-derived vegetation growth trend in temperate and boreal Eurasia from 1982 to 2006 *Glob. Change Biol.* **17** 3228–39

Rawlins M A *et al* 2010 Analysis of the arctic system for freshwater cycle intensification: observations and expectations *J. Clim.* **23** 5715–37

Reager J T and Famiglietti J S 2009 Global terrestrial water storage capacity and flood potential using GRACE *Geophys. Res. Lett.* **36** L23402

Rodell M, Velicogna I and Famiglietti J S 2009 Satellite-based estimates of groundwater depletion in India *Nature* **460** 999–1002

Saito K, Kimoto M, Zhang T, Takata K and Emori S 2007 Evaluating a high-resolution climate model: simulated hydrothermal regimes in frozen ground regions and their change under the global warming scenario *J. Geophys. Res.* **112** F02S11

Schwalm C R *et al* 2010 Assimilation exceeds respiration sensitivity to drought: a FLUXNET synthesis *Glob. Change Biol.* **16** 657–70

Serreze M C, Barrett A P, Slater A G, Woodgate R a, Aagaard K, Lammers R B, Steele M, Moritz R, Meredith M and Lee C M 2006 The large-scale freshwater cycle of the Arctic *J. Geophys. Res.* **111** C11010

Sillmann J, Kharin V V, Zwiers F W, Zhang X and Bronaugh D 2013 Climate extremes indices in the CMIP5 multimodel ensemble: II. Future climate projections *J. Geophys. Res. Atmos.* **118** 2473–93

Soja A J, Tchebakova N M, French N H F, Flannigan M D, Shugart H H, Stocks B J, Sukhinin A I, Parfenova E I, Chapin F S and Stackhouse P W 2007 Climate-induced boreal forest change: predictions versus current observations *Glob. Planet. Change* **56** 274–96

Swenson S, Chambers D and Wahr J 2008 Estimating geocenter variations from a combination of GRACE and ocean model output *J. Geophys. Res.* **113** B08410

Swenson S, Yeh P J-F, Wahr J and Famiglietti J 2006 A comparison of terrestrial water storage variations from GRACE with *in situ* measurements from Illinois *Geophys. Res. Lett.* **33** L16401

Tang Q and Leng G 2012 Damped summer warming accompanied with cloud cover increase over Eurasia from 1982 to 2009 *Environ. Res. Lett.* **7** 014004

Tapley B D, Bettadpur S, Ries J C, Thompson P F and Watkins M M 2004 GRACE measurements of mass variability in the Earth system *Science* **305** 503–5

Tchebakova N M, Parfenova E and Soja A J 2009 The effects of climate, permafrost and fire on vegetation change in Siberia in a changing climate *Environ. Res. Lett.* **4** 045013

Tei S, Yonenobu H, Sugimoto A, Ohta T and Maximov T C 2015 Reconstructed summer Palmer Drought Severity Index since 1850 AD based on δ13C of larch tree rings in eastern Siberia *J. Hydrol.* **529** 442–8

Thomas A C, Reager J T, Famiglietti J S and Rodell M 2014 A GRACE-based water storage deficit approach for hydrological drought characterization *Geophys. Res. Lett.* **41** 1537–45

Velicogna I, Tong J, Zhang T and Kimball J S 2012 Increasing subsurface water storage in discontinuous permafrost areas of the Lena River basin, Eurasia, detected from GRACE *Geophys. Res. Lett.* **39** L09403

Vicente-Serrano S M *et al* 2013 Response of vegetation to drought time-scales across global land biomes *Proc. Natl Acad. Sci. USA* **110** 52–7

Vicente-Serrano S M, Beguería S and López-Moreno J I 2010 A multiscalar drought index sensitive to global warming: the standardized precipitation evapotranspiration index *J. Clim.* **23** 1696–718

Wahr J, Molenaar M and Bryan F 1998 Time variability of the Earth's gravity field: hydrological and oceanic effects and their possible detection using GRACE *J. Geophys. Res.* **103** 30205–29

Walker D A *et al* 2009 Spatial and temporal patterns of greenness on the Yamal Peninsula, Russia: interactions of ecological and social factors affecting the Arctic normalized difference vegetation index *Environ. Res. Lett.* **4** 045004

Walker X and Johnstone J F 2014 Widespread negative correlations between black spruce growth and temperature across topographic moisture gradients in the boreal forest *Environ. Res. Lett.* **9** 064016

Wang M and Overland J E 2004 Detecting Arctic climate change using KÖppen climate classification *Clim. Change* **67** 43–62

Yang Y, Long D, Guan H, Scanlon B R, Simmons C T, Jiang L and Xu X 2014 GRACE satellite observed hydrological controls on interannual and seasonal variability in surface greenness over mainland Australia *J. Geophys. Res. Biogeosciences* **119** 2245–60

Yi C *et al* 2010 Climate control of terrestrial carbon exchange across biomes and continents *Environ. Res. Lett.* **5** 034007

Yi Y, Kimball J S, Jones L a, Reichle R H, Nemani R and Margolis H A 2013 Recent climate and fire disturbance impacts on boreal and arctic ecosystem productivity estimated using a satellite-based terrestrial carbon flux model *J. Geophys. Res. Biogeosciences* **118** 606–22

Yi Y, Kimball J S and Reichle R H 2014 Spring hydrology determines summer net carbon uptake in Northern ecosystems *Environ. Res. Lett.* **9** 064003

Zhang K, Kimball J S, Hogg E H, Zhao M, Oechel W C, Cassano J J and Running S W 2008 Satellite-based model detection of recent climate-driven changes in Northern high-latitude vegetation productivity *J. Geophys. Res.* **113** G03033

Zhang K, Kimball J S, McDonald K C, Cassano J J and Running S W 2007 Impacts of large-scale oscillations on pan-Arctic terrestrial net primary production *Geophys. Res. Lett.* **34** L21403

Zhang K, Kimball J S, Mu Q, Jones L A, Goetz S J and Running S W 2009 Satellite based analysis of Northern ET trends and associated changes in the regional water balance from 1983 to 2005 *J. Hydrol.* **379** 92–110

Zhang T *et al* 2005 Spatial and temporal variability in active layer thickness over the Russian Arctic drainage basin *J. Geophys. Res.* **110** D16101

Zhang X, He J, Zhang J, Polyakov I, Gerdes R, Inoue J and Wu P 2012 Enhanced poleward moisture transport and amplified Northern high-latitude wetting trend *Nat. Clim. Change* **3** 47–51

Zhou L, Tucker C J, Kaufmann R K, Slayback D, Shabanov N V and Myneni R B 2001 Variations in Northern vegetation activity inferred from satellite data of vegetation index during 1981–1999 *J. Geophys. Res.* **106** 20069